JACS
JOURNAL OF THE AMERICAN CHEMICAL SOCIETY

COMMUNICATION

pubs.acs.org/JACS

Effect of Oxygen on the Electronic Structure of Highly Crystalline Picene Films

Ying Wang,*[,†] Simone Di Motta,[‡] Fabrizia Negri,*[,‡] and Rainer Friedlein*[,†]

[†]School of Materials Science, Japan Advanced Institute of Science and Technology, 1-1 Asahidai, Nomi, Ishikawa 923-1292, Japan

[‡]Università degli Studi di Bologna, Dipartimento di Chimica "G. Ciamician", Via F. Selmi, 2 and INSTM, UdR Bologna, I - 40126 Bologna, Italy

Supporting Information

ABSTRACT: The electronic structure of highly crystalline picene films with a standing-up orientation grown epitaxially on the Ag(110) surface was investigated. Upon exposure to oxgen gas, O_2 molecules incorporate at the interstitial sites within the $a-b$ plane of the film. Features related to the highest three occupied molecular orbitals shift toward a lower binding energy which results in the inactivation of traps and the reduction of the charge injection barrier by about 1 eV. It is suggested that the highest two picene orbitals are inverted due to the strong interactions between the singly occupied oxygen π orbital and the highest occupied orbital of picene.

Organic semiconductors exhibit unique physical and electronic properties which make them promising materials for applications in electronic devices.[1−4] Understanding the fundamental processes governing the charge transport remains a central issue for the improvement of organic-based devices. In general, electronic properties of most organic semiconductors are highly sensitive to the atmospheric environment and in particular to the exposure to oxygen (O_2). For example, oxidation of crystalline rubrene has a significant effect on the charge transport since impurities form new states within the original gap.[5] As found for a number of rather small molecules and polymers,[6−8] molecular oxgyen can also adsorb physically and cause p-doping of the organic semiconductors which has a pronounced effect on the conductivity.[9] Although much effort has been devoted to studying the effects associated with the incorporation or reaction of oxygen species on the transport characteristics of organic semiconductors,[10−15] progress is still limited since the underlying fundamental mechanisms are only partially understood.

An isomer of pentacene called picene, the molecular structure of which is depicted in the inset of Figure 1, has recently shown some remarkable and unusual transport properties.[16−18] As active materials in organic field-effect transistors, pristine thin films exhibit a hole mobility of more than 3 $cm^2/(V\ s)$. More fascinating, the mobility is enhanced up to 5 $cm^2/(V\ s)$ upon exposure to O_2 gas at 500 Torr.[17,18] These unique phenomena inspired us to study the changes of electronic structure induced by the interaction between oxygen and picene. Here the epitaxial growth is reported of highly crystalline picene films with a standing-up orientation on the Ag(110) surface that provide an ideal platform for the study of the electronic structure. The

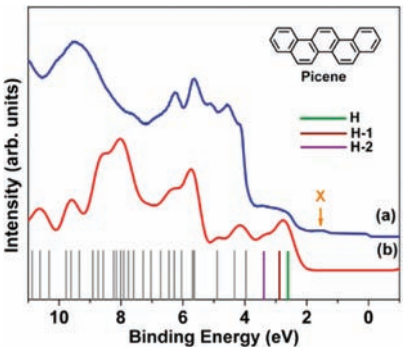

Figure 1. (a) UPS spectrum of the picene/Ag(110) multilayer film measured with respect to E_F and (b) a simulated spectrum derived from calculated molecular orbital energies, shown at the bottom. H, H-1, and H-2 denote the three highest occupied molecular orbitals, HOMO, HOMO-1, and HOMO-2, respectively. Feature "X" is attributed to trapping states (see text). The molecular structure of picene is shown in the inset.

Ag(110) surface was chosen due to its low symmetry and the good matching of multiples of lattice parameters with those reported for the bulk[16] of picene. Changes of electronic properties caused by the incorporation of molecular oxygen into the interstitial sites within the film were studied by ultraviolet photoelectron spectroscopy (UPS) and density-functional-theory (DFT) based calculations.

Upon deposition of picene on Ag(110), the work function (φ) decreases by about 0.60 ± 0.05 eV to a value of φ = 4.25 ± 0.10 eV. Saturation at a nominal film thickness of about 13.8 Å is consistent with the completion of the first molecular layer (1 ML) with a "standing-up" molecular orientation. With increasing thickness, the UPS valence band spectrum changes (see the Supporting Information (SI)). The intensity of the feature related to the Ag (3d) band is gradually suppressed. As shown for the spectrum of the pristine multilayer film in Figure 1, several adsorbate-induced spectral features appear in the binding energy range between 2 and 8 eV. The separation between these features corresponds well to the spacing of B3LYP/6-31G* calculated energy levels[19] of the picene molecule (shown at the bottom) which in turn agree with those of recent calculations.[20] The sharpness of the features between about 4 and 6 eV indicates the formation of highly ordered thin films on Ag(110). In the

Received: May 2, 2011
Published: June 07, 2011

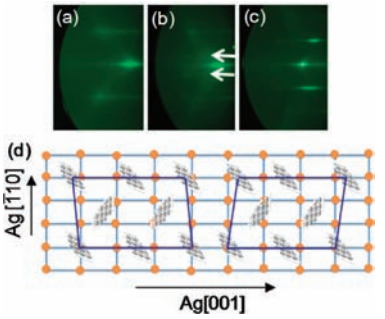

Figure 2. RHEED pattern of (a) the Ag(110) surface and (b) picene ML film on Ag(110), with the electron beam directed along the Ag [001] direction and of (c) a picene ML film on Ag(110), with the electron beam directed along the Ag [$\bar{1}$10] direction. (d) Schematic representation of the picene ML unit cell with respect to the underlying Ag(110) lattice.

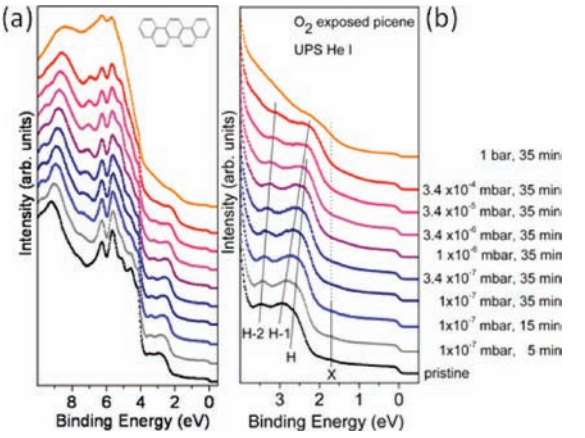

Figure 3. Evolution of the valence band photoelectron spectra of the picene/Ag(110) multilayer film as a function of the oxygen exposure time and pressure, in a wider (a) and narrower (b) range. The corresponding spectra of the pristine picene film are inclued for comparison.

low-binding energy region of the pristine multilayer film shown in Figure 1, spectral features at about 2.6, 2.96, and 3.5 eV, denoted H, H-1, and H-2, relate to the three highest occupied molecular orbitals, HOMO, HOMO-1, and HOMO-2, respectively. Additionally, a weak spectral feature centered at the binding energy of 1.55 eV, denoted X, may be recognized as part of a tail at the low-binding energy side of the HOMO. This feature is certainly a signature of trapping states caused by structural defects associated with the formation of the multilayer and not by impurities since it is not detected for thicknesses below 16 Å. At the Fermi level, E_F, a step-like feature is visible even for the multilayer films with a nominal thickness of about 35 Å. Since multilayer films are not expected to be metallic, electronic states at E_F should derive from the nonvanishing contribution of the substrate or from interfacial states associated with the first layer. It is therefore concluded that the growth proceeds in multilayer islands. This conclusion is also supported by Atomic Force Microscopy measurements (see the SI) showing an island-like multilayer film with a profile containing protrusions up to 10 nm deep.

Reflection high-energy electron diffraction (RHEED) images of the Ag(110) surface and of a monolayer picene film are shown in Figure 2a and b, respectively. The patterns obtained with the electron beam directed along the Ag[001] crystallographic direction represent the reciprocal periodicity along the [$\bar{1}$11] direction. Upon deposition of the molecules, additional streaks with a spacing of one-third of the original ones appear as indicated with white arrows. The clear RHEED pattern comprising narrow and enlongated side streaks is both an indication of a high degree of crystallinity of the picene films and of a good expitaxial relationship with the Ag(110) surface. In the [$\bar{1}$10] direction, the picene unit cell is three times larger than that of the substrate. In the [001] direction (Figure 2c), no additional streaks related to the picene lattice are observed. Since the lattice constants in the relevant $a-b$ plane of bulk picene[16] would match with multiples of those of the Ag(110) surface, additional streaks should be expected in the case of a rectangular thin film unit cell. On the other hand, small deviations of 2° to 4° of the unit cell vector from the [$\bar{1}$10] direction would lead to the observed pattern and a monoclinic film structure. A model of the as-derived in-plane unit cells of coexisting twin domains is shown in Figure 2d. The length of the unit cell vectors within the $a-b$ plane of 8.79 and 12.12 Å is consistent with a unit cell of an epitaxial monolayer containing four molecules. In subsequent layers, this ML unit cell naturally gives rise to a unit cell that would be half the size in the [001] direction once the contact to the Ag surface is lost. Additional confidence in the proposed model is found in the fact that the nearest-neigbour molecular distance of about 5.16 Å is similar to that in bulk material.

Note that picene thin films on Ag(110) exhibit a standing-up orientation from the very beginning. This is markedly distinct to monolayer thin films of pentacene and of other aromatic molecules on the same surface where the molecular plane is parallel to the substrate surface.[21,22] The orientational difference may indicate a particular molecule−substrate interaction governed by epitaxy conditions. For the following discussion related to the effect of oxygen on the electronic properties, details of the structure model are important as there is a strong resemblance of the thin film structure with that of the bulk material. In particular, O_2 molecules may occupy interstitial sites *within the $a-b$ plane* similar to those used by K-atoms in superconducting K-intercalated picene.[16] It is logical to assume that the oxygen guest species would be in the form of weakly interacting oxygen molecules since other forms of oxygen may not undergo reversible reactions. Covalent bonds to the picene molecules would have already formed *prior* to the introduction of the molecules into the vacuum systems. Due to the particular w-shaped chemical structure, picene molecules are actually predicted to be resistant against quinone formation.

In Figure 3 are shown UPS spectra obtained after stepwise exposure to oxygen gas, at selected exposure times. With increasing partial pressure, φ increases steadily by a final amout of about 0.7 ± 0.05 eV that is obtained after exposure to 1 bar for 35 min. In the valence band region shown in Figure 3a and b, spectral features centered at about 4.60, 5.10, 5.64, and 6.26 eV remain pinned to E_F while others at 7.65 and 9.20 eV and those in the range of 2−4 eV, denoted the H, H-1, and H-2, shift toward a lower binding energy. Even more, as clearly visible in Figure 3b, the shift is different for each of the latter three π levels. Such orbital-specific properties must reflect special interactions between picene π orbitals and incorporated oxygen atoms within the $a-b$ plane of the film. The picene films remain ordered after exposure to oxygen gas pressures of up to at least 3.4 × 10^{-4}

dx.doi.org/10.1021/ja204011j |*J. Am. Chem. Soc.* 2011, 133, 10054–10057

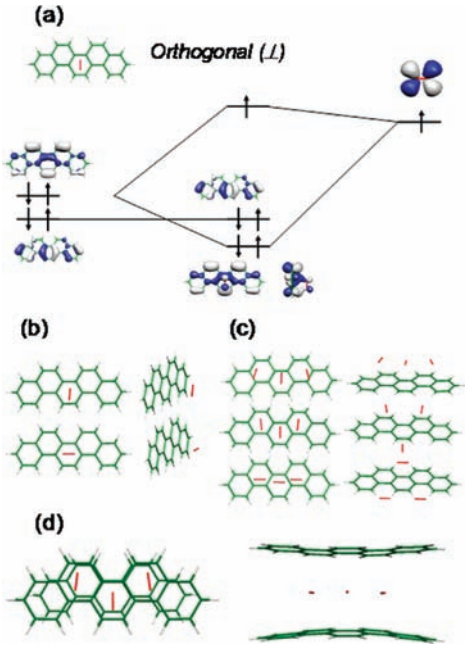

Figure 4. (a) Qualitative orbital interaction scheme for a picene−O_2 complex maximizing the interaction between oxygen and the HOMO orbital of picene. To simplify the scheme only one of the two singly occupied orbitals of O_2 is shown. Quantum-chemically optimized structures determined for several complexes of oxygen with picene: (b) picene + O_2 (// and ⊥ complexes); (c) picene + three O_2 (// and ⊥ complexes, with the ⊥ complex featuring the three oxygens on the same side being the most stable structure); and (d) three ⊥ O_2 sandwiched between two picenes.

mbar which is proven by the persistence of the RHEED patterns (not shown) characteristic of the pristine film. This indicates that the O_2 molecules are incorporated at interstitial sites allowing the above-mentioned unique electronic interactions. Note that the unit cell of pristine picene is significantly larger than those of herringbone-stacked oligoacene films where intercalants sit in between molecular layers.[23] The increase of φ upon exposure to oxygen gas and the pinning of the majority of electronic levels to the Fermi level are consistent with a *p*-type doping of the films related to an effective partial electron transfer from the molecules to the oxygen atoms. In this picture, the pinning level may be related to the now partially unoccupied HOMO, and the change of φ could reflect changes of the chemical potential of the films as it does for alkaline-metal intercalated films of polyaromatic hydrocarbons.[24]

As the transport of positive charge carriers in organic materials does occur mainly *via* electronic states related to the HOMO, a more careful look at the associated spectral features and their behavior upon exposure to oxygen gas is required. As shown in Figure 3b, in pristine picene films, H and H-1 are split by only about 0.3 eV. While both features shift toward a lower binding energy, the one related to the HOMO-1 exhibits a much larger shift surpassing the original HOMO at exposures in the 10^{-4} mbar range. The transfer of spectral weight toward a lower binding energy continues upon exposure to oxygen gas at ambient conditions (1 bar for 35 min). Even if it is difficult to distinguish individual features from the observed trends, it may then be concluded that (i) the original HOMO-1 becomes itself the highest occupied orbital (ii) at energies in the vicinity of the original trapping states related to the feature X at 1.55 eV. The appearance of a new frontier orbital at energies close to the feature X has important consequences for the transport of positive charge carriers: Structural traps related to the former HOMO or any other traps associated with X may then become inactive since the charge transport will occur *via* states related to the original HOMO-1. This explains why picene thin films exhibit a higher hole drift mobility under ambient conditions as compared to the pristine material in vacuum.[18] Note that apart from the improved charge transport in the bulk, also the barrier for hole injection from the metal to the film is reduced by almost 1 eV which leads to a higher performance by devices as well.[25]

The inversion of frontier orbitals due to the interaction with molecular oxygen is a strong effect that deserves particular attention. In the case of free aromatic molecules, theoretical studies agree in predicting a weak interaction dominated by van der Waals forces and a preferential orientation of the O_2 molecular axis parallel to the molecular plane.[26,27] With regard to the aromatic sextet underlying aromatic hydrocarbon compounds, two possible orientations of O_2 parallel to the molecular plane may be called *orthogonal* (⊥) and *parallel* (//) by referring to the fact that in // the O_2 molecules lies along a line connecting two opposite carbon atoms while in ⊥ it is perpendicular to such a line. Guided by the oxygen orientation, the singly occupied π orbital of oxygen, with lobes perpendicular to the molecular plane, interacts only with one of the two highest occupied picene orbitals. The orbital interacting with oxygen is slightly mixed with the O_2 π orbital and pushed toward a lower energy while the other one is not affected (see SI for a discussion of the case of benzene). For complexes maximizing the interaction with the picene HOMO, oxygen molecules will be in the ⊥ position. For this case, as shown in Figure 4a, it is the HOMO which is lowered. If the interaction is sufficiently strong, or if the distance between oxygen and picene molecules is forced to be reduced (as compared to the gas phase), this eventually may lead to an inversion of the original HOMO and HOMO-1 obitals of picene.

In Figure 4b and c are shown the results of calculations on complexes with either one or three oxygen molecules, respectively. All the computed complexes between oxygen molecules in their triplet state and picene are characterized by intermolecular distances between oxygen and picene on the order of 3.2 Å. The ⊥ complex with three O_2 molecules on the same side is the most stable (by about 2.6 kcal). For these calculated structures, the energetic effect on the picene HOMO orbital is modest and does not lead to the experimentally observed proximity of the HOMO and HOMO-1 orbitals. The behavior changes for three oxygen molecules sandwiched in ⊥ positions between two picene molecules, the optimized structure shown in Figure 4c. For appropriate distances between the two picene molecules close to those in the solid state, the interaction with oxygen leads to a strong displacement of the HOMO orbital. As the geometry optimization for the free complex reaches the minimum energy, the interaction becomes weaker and the energy displacement of the HOMO is reduced. Nevertheless, the calculated results are in qualitative agreement with the experimental observations with respect to the orbital inversion providing details of the exact mechanism behind the peculiar electronic changes following the incorporation of molecular oxygen within the *a*−*b* plane of the picene crystal.

In summary, highly crystalline picene films with a standing-up orientation were grown epitaxially on the Ag(110) surface. Upon exposure to oxygen gas, the O_2 molecules incorporate at

interstitial sites within the $a-b$ plane consisting of layers of standing molecules. Energy levels related to the highest three occupied molecular orbitals shift toward a lower binding energy which results in the inactivation of traps and the reduction of the charge injection barrier by about 1 eV. Additionally, strong interactions between the singly occupied oxygen π orbital and the highest occupied orbital of picene may lead to an inversion of the original HOMO and HOMO-1. The appearance of a new frontier orbital and the inactivation of traps explain the higher hole mobility of picene OFETs under an oxygen atmosphere as compared to those made of pristine material in vacuum. This result is significant for the understanding and control of environmental factors as needed for applications in organic devices.

■ ASSOCIATED CONTENT

Supporting Information. Details concerning the sample preparation, UPS and RHEED measurements, quantum-chemical calculations as well as figures showing UPS spectra as a function of the nominal picene film thickness, and an Atomic Force Microscopy image of a multilayer film are included in the Supporting Information. This material is available free of charge via the Internet at http://pubs.acs.org.

■ AUTHOR INFORMATION

Corresponding Author
wang-y@jaist.ac.jp; fabrizia.negri@unibo.it; friedl@jaist.ac.jp

■ ACKNOWLEDGMENT

We thank A. Fujiwara (JASRI/Spring 8 Synchrotron Radiation Facility, Japan) and Y. Yamada-Takamura (JAIST) for discussions and help. This work has been supported by Special Coordination Funds for Promoting Science and Technology, commissioned by MEXT, Japan, and by the MAZDA and MARUBUN Foundations. F.N. acknowledges financial support by Italian MIUR, PRIN Project 2008 JKBBK4 "Tracking ultrafast photoinduced intra- and intermolecular processes in natural and artificial photosensors".

■ REFERENCES

(1) Huitema, H. E. A.; Gelinck, G. H.; van der Putten, J. B. P. H.; Kuijk, K. E.; Hart, C. M.; Cantatore, E.; Herwig, P. T.; van Breemen, A. J. J. M.; de Leeuw, D. M. *Nature* **2001**, *414*, 599.
(2) Zaumseil, J.; Sirringhaus, H. *Chem. Rev.* **2007**, *107*, 1296–1323.
(3) Wang, Y.; Acton, O.; Ting, G.; Weidner, T.; Shamberge, P. J.; Ma, H.; Ohuchi, F. S.; Castner, D. G.; Jen, A. K.-Y. *Org. Electr.* **2010**, *11*, 1066–1073.
(4) Gao, X. K.; Wang, Y.; Yang, X. D.; Liu, Y. Q.; Qiu, W. F.; Wu, W. P.; Zhang, H. J.; Qi, T.; Liu, Y.; Lu, K.; Du, C. Y.; Shuai, Z. G.; Yu, G.; Zhu, D. B. *Adv. Mater.* **2007**, *19*, 3037–3042.
(5) Käfer, D.; Witte, G. *Phys. Chem. Chem. Phys.* **2005**, *7*, 2850–2853.
(6) Abdou, M. S. A.; Orfino, F. P.; Son, Y.; Holdcroft, S. *J. Am. Chem. Soc.* **1997**, *119*, 4518–4524.
(7) Collins, P. G.; Bradley, K.; Ishigami, M.; Zettle, A. *Science* **2000**, *287*, 1801–1804.
(8) Meijer, E. J.; Detcheverry, C.; Baesjou, P. J.; van Veenendaal, E.; de Leeuw, D. M.; Klapwijk, T. M. *J. Appl. Phys.* **2003**, *93*, 4831–4835.
(9) Anthopoulos, T. C.; Shafai, T. S. *Appl. Phys. Lett.* **2003**, *82*, 1628–1630.
(10) Mitrofanov, O.; Lang, D. V.; Kloc, C.; Wikberg, J. M.; Siegrist, T.; So, W.-Y.; Sergent, M. A.; Ramirez, A. P. *Phys. Rev. Lett.* **2006**, *97*, 166601.
(11) Lu, C.-K.; Meng, H.-F. *Phys. Rev. B* **2007**, *75*, 235206.
(12) Tanaka, Y.; Kanai, K.; Ouchi, Y.; Seki, K. *Chem. Phys. Lett.* **2007**, *441*, 63–67.
(13) Vollmer, A.; Jurchescu, O. D.; Arfaoui, I.; Salzmann, I.; Palstra, T. T. M.; Rudolf, P.; Niemax, J.; Pflaum, J.; Rabe, J. P.; Koch, N. *Eur. Phys. J. E* **2005**, *17*, 339–343.
(14) Song, X.; Wang, L.; Fan, Q.; Wu, Y.; Wang, H.; Liu, C. *Appl. Phys. Lett.* **2010**, *97*, 032106.
(15) Najafov, H.; Mastrogiovanni, D.; Garfunkel, E.; Feldman, L. C.; Podzorov, V. *Adv. Mater.* **2011**, *23*, 981–985.
(16) Mitsuhashi, R.; Suzuki, Y.; Yamanari, Y.; Mitamura, H.; Kambe, T.; Ikeda, N.; Okamoto, H.; Fujiwara, A.; Yamaji, M.; Kawasaki, N.; Maniwa, Y.; Kubozono, Y. *Nature* **2010**, *464*, 76–79.
(17) Okamoto, H.; Kawasaki, N.; Kaji, Y.; Kubozono, Y.; Fujiwara, A.; Yamaji, M. *J. Am. Chem. Soc.* **2008**, *130*, 10470–10471.
(18) Kawasaki, N.; Kubozono, Y.; Okamoto, H.; Fujiwara, A.; Yamaji, M. *Appl. Phys. Lett.* **2009**, *94*, 043310.
(19) Kuritka, I.; Negri, F.; Brancolini, F.; Suess, C.; Salaneck, W. R.; Friedlein, R. *J. Phys. Chem. B* **2006**, *110*, 19023–19030.
(20) Roth, F.; Gatti, M.; Cudazzo, P.; Grobosch, M.; Mahns, B.; Büchner, B.; Rubio, A.; Knupfer, M. *New J. Phys.* **2010**, *12*, 103036.
(21) Gao, L.; Deng, Z. T.; Ji, W.; Lin, X.; Cheng, Z. H.; He, X. B.; Shi, D. X.; Gao, H.-J. *Phys. Rev. B* **2006**, *73*, 075424.
(22) Craciun, M. F.; Giovannetti, G.; Rogge, S.; Brocks, G.; Morpurgo, A. F.; van den Brink, J. *Phys. Rev. B* **2009**, *79*, 125116.
(23) Anders, H.; Johan, B.; Sven, S. *Phys. Rev. B* **2006**, *73*, 184114.
(24) Friedlein, R.; Crispin, X.; Pickholz, M.; Keil, M.; Stafström, S.; Salaneck, W. R. *Chem. Phys. Lett.* **2002**, *354*, 389–391.
(25) Di, C.; Liu, Y.; Yu, G.; Zhu, D. *Acc. Chem. Res.* **2009**, *42*, 1573–158.
(26) Granucci, G.; Persico, M. *Chem. Phys. Lett.* **1993**, *205*, 331–336.
(27) Weselowski, T. A.; Parisel, O.; Ellinger, Y.; Weber, J. *J. Phys. Chem. A* **1997**, *101*, 7818.